Paper

Application of lubricants structure on ophthalmic lens

Nobuyuki Tadokoro[1]*, Supaporn Pannakarn[2], Jutathap Wisuthtatip[2], Sureerat Kunchoo[2], Veeraphat Parnich[2], Kenji Takashiba[2], Koji Shimizu[2], and Hisashi Higuchi[2]
[1]*Lens Technology Center, VC Company, HOYA Corporation*
1-1 Kowada, Akiruno-shi, Tokyo 190-0151, Japan
[2]*PL Technical Depertment, HOYA Lens Thailand*
202 Moo1, Banwah (Hi-Tech) Industrial Estate (Epz), Banlane, Bang Pa-in, Ayutthaya 13160, Thailand
**nobuyuki.tadokoro@hoyavc.com*

(Received: October 3, 2010; Accepted: January 18, 2011)

In this paper, novel approaches to the study of the relationship between the chemical structures and the wear properties of lubricants on an ophthalmic lens by various analytical methods are described. The X-ray damage of lubricants by X-ray photoelectron spectroscopy (XPS) depends upon the lubricant structure. Further, the lubricant structure influences the wear properties. In particular, the experimentally observed X-ray damage and wear properties indicate that the straight linear chain structure with no side chain structure ((-CF_2-CF_2-O-)m-(CF_2-O-)n) is stronger than that with the side chain structure ((-CF (CF_3)-CF_2-O-)m). This result suggests that the investigation of X-ray damage by XPS is equivalent to an examination of the strength of the wear characteristic. The abovementioned methods are suitable for studying the durability of lubricants on ophthalmic lenses.

1. Introduction

Perfluoropolyether (PFPE) lubricants have been widely used to improve tribological performance and wear properties. Several investigations of a magnetic disk surface on which PFPE lubricants are present have been carried out by ellipsometry [1-3], grazing-angle X-ray reflectivity (XRR) [3], Fourier transform infrared spectroscopy (FT-IR) [3, 4], X-ray photoelectron spectroscopy (XPS) [3, 5, 6], atomic force microscopy (AFM) [1, 2, 6, 7, 8], and secondary ion mass spectrometry (SIMS) [6, 9, 10]. In general, the lubricant thickness or lubricant formation has been evaluated by ellipsometry, XPS, FT-IR, XRR, and SIMS. To our knowledge, previous experimental studies have been confined to magnetic disks, magnetic heads, and protective layers. Modern lubricants have been used to improve the tribological performance of ophthalmic lenses; it is especially important to control the distribution of lubricants in order to (1) maintain the wear properties on the lens surface and (2) protect the surface from dirt. A few investigations have been carried out on the lubricant properties of ophthalmic lenses [11, 12]. The purpose of the present study is to examine the relationship between the structure of lubricant films and the wear properties on the lens surface.

2. Experimental

Commercial ophthalmic lenses were used in this study. Detailed estimations of lubricants were carried out directly on silicon wafer in order to avoid the influence of surface curvature, roughness, or amorphous states of actual ophthalmic lenses. The structures of the ophthalmic lenses were as follows: a hard coating underlayer (HC) on the plastic lens substrate was created by dip-coating methods. Anti-reflection (AR) coating layers, such as the sandwich structures between low-index material and high-index material, were deposited by vacuum deposition methods after the HC underlayer was cleaned by ultrasonic washing using detergent and deionized water. The PFPE lubricants, which were also commercial products, were deposited over the AR coating layers by the vacuum deposition methods. The main structure of lubricants A has (-CF (CF_3)-CF_2-O-)m, the main structure of lubricants B and lubricants C has (-CF_2-CF_2-O-)m-(CF_2-O-)n. The difference between lubricants B and lubricants C is the end group structure such as lubricants B is terminated by -CH_3, and lubricants C is terminated -CH_2-CF_3. The surface morphology and the lubricant film distribution were examined by atomic force microscopy (AFM; Asylum Research, Molecule Force Microscope System MFP-3D). The film thickness, morphology of the cross section, and elemental analysis were used by

transmission electron microscopy (TEM-EDS; JEOL, JEM-200FX-2). The film thickness and the coverage ratio of the lubricant were measured by X-ray photoelectron spectroscopy (XPS; Physical Electronics, PHI ESCA5400MC). Structure analysis was conducted by time-of-flight secondary ion mass spectrometry (TOF-SIMS; ULVAC-PHI, PHI TRIFT-4) and XPS. The wear properties of lubricants were evaluated by contact angle measurement (Kyowa Interface Science Co., Ltd.; Contact angle meter, model CA-D) and by the use of an abrasion tester (Shinto Scientific Co., Ltd.; Heidon Tribogear, Type 30S). The abrasion test was rubbed in the Dusper K3(Ozu corp.) to have wrapped around the eraser under the condition of 2 kg weight and 600 strokes.

3. Results and discussion

Fig.1 shows a TEM photograph of a lubricant on a silicon wafer. The thickness of the lubricant layer was estimated to be 2.6 nm. Table 1 summarized the lubricant film thickness and coverage ratio. These data indicate that both the film thicknesses and the coverage ratios were almost identical across all films. Here, we directly measured the film thickness by TEM. XPS was used the analysis of coverage ratio and film thickness by the island model of Kimachi methods [5]. Despite the fact that the lubricant layer was comprised of organic materials, the existence of the lubricant film was directly observed and the film thickness was successfully measured by TEM. Generally, the issue of TEM measurement is sample damage by electron beam. For the reason of successful measurement by TEM, it seems that the lubricant damage of ophthalmic lens is stronger than that of the magnetic disk for electron beam. And also, we recognized fluorine element in this area by TEM-EDS.

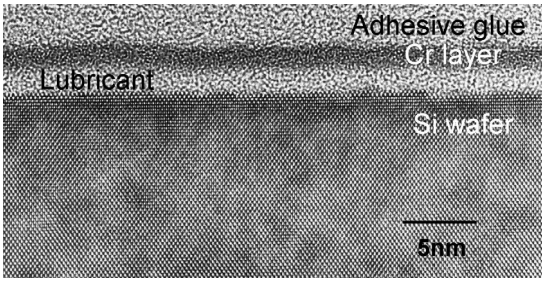

Fig.1. TEM cross-sectional photograph (adhesive glue/Cr protectant layer/lubricant/Si wafer).

Table 1. Film thicknesses by TEM & XPS, and coverage ratios as determined by XPS.

	Lub. Film thickness(nm)	Lub. Film Coverage(%)
Sample-A	2.4-2.9	98 over
Sample-B	2.3-2.7	98 over
Sample-C	2.3-2.7	98 over

Fig.2 shows the X-ray damage ratio of F1s spectra as a function of X-ray exposure time under the condition of X-ray power 300W and Mg-Kα source by XPS. Fig.3 shows the initial structure of the mass spectra of positive fragment ions, as obtained by TOF-SIMS (upper spectrum: sample A, middle spectrum: sample B, lower spectrum: sample C). Fig.4 shows the changing chemical structure of C1s for sample A as a function of exposure time (initial structure shown for reference, structure after 30 min, and structure after 60 min), as determined by XPS. Fig.5 shows the mass spectra of negative fragment ions for sample A, as obtained by TOF-SIMS (upper spectrum: initial, lower spectrum: after 60 min, obtained by XPS).

From fig.2, we found that the X-ray damage in the case of sample A is greater than that in the case of sample B and sample C. In the case of sample B and sample C, the lubricant component of fluorine remained on the surface; fluorine was presented on approximately 80% on the surface after 60 min of exposure to X-ray. On the other hand, the lubricant component of sample A decreased by approximately 40% after exposure for 60 min.

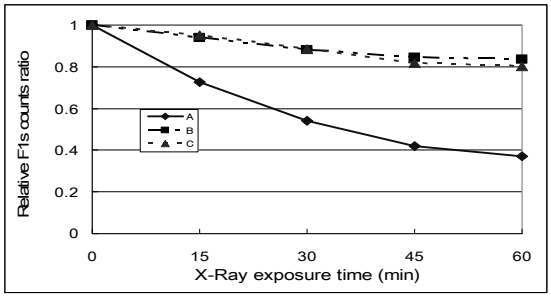

Fig.2. Relationship between F1s intensity and X-ray exposure time during XPS.

On the basis of the initial structures shown in Fig.3 and Fig.5, it is concluded that the main structure of sample A has a side chain structure (-CF (CF_3)-CF_2-O-)m, similar to that in Fombline Y or Krytox. This periodic relation of 166 amu (C_3F_6O) continues up till mass numbers of approximately 5000 amu. In the case of magnetic disks, the high molecular structure of the lubricants was realized and maintained by dip coating or spin coating. However, the ophthalmic lens of lubricants was deposited by lamp heating methods into vacuum. Nevertheless, some main structure of lubricants was contained high-polymeric structures.

On the other hand, the main structures of sample B and sample C have a straight chain structure without the side chain structures (-CF_2-CF_2-O-)m-(CF_2-O-)n, similar to the main

structure of Fombline Z. From fig.4 and fig.5, we found that the main chemical structure of lubricants for sample-A is decreasing and destroying as a function of exposure time by XPS.

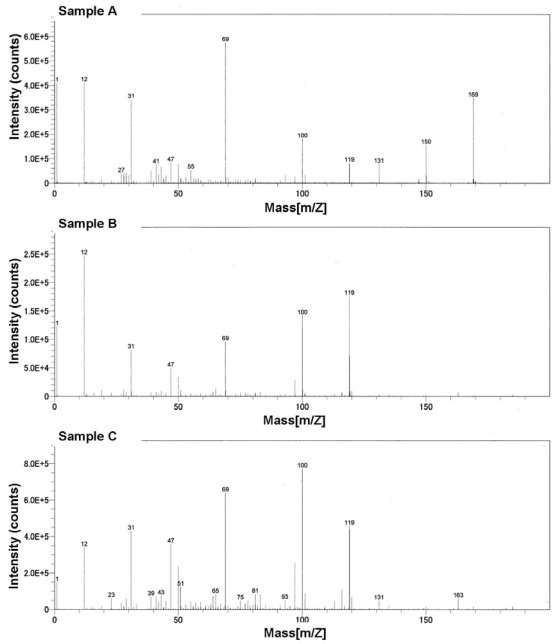

Fig.3. Initial structure of the mass spectra of positive fragment ions, as determined by TOF-SIMS (upper spectrum: sample A, middle spectrum: sample B, lower spectrum: sample C).

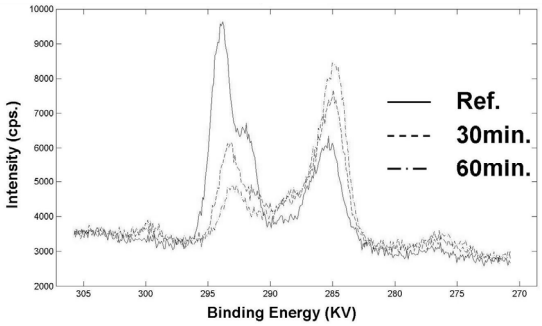

Fig.4. Changing chemical structure of C1s for sample A as a function of exposure time (initial structure, shown for reference; structure after 30 min; and structure after 60 min), as determined by XPS. The analysis time of C1s spectrum obtained was carried out 3.4min approximately.

These observations suggest that the straight chain structure of (-CF_2-CF_2-O-)m-(CF_2-O-)n is more robust to X-ray damage during XPS than the side chain structure (-CF (CF_3)-CF_2-O-)m. We attribute this difference in the strength of the structures to the presence or absence of the chemical structure of the side chain. TEM or XPS measurement reveals that the film thickness of the lubricants is 2-3 nm. According to Tani [7], he found double steps on the lubricant film with 2.9nm thickness that was almost completely cover the surface by the mean molecular radius of gyration with coil of lubricant molecular. Therefore, it seems that the 2-3 coils of lubricant molecular have been stacked on the surface of the ophthalmic lens.

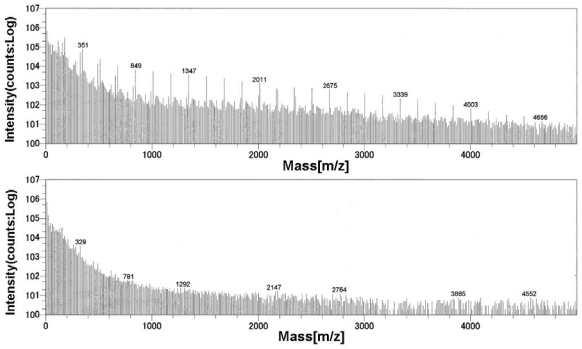

Fig.5. Mass spectra of negative fragment ions for sample A, as determined by TOF-SIMS (upper spectrum: initial, lower spectrum: after 60 min X-ray exposure by XPS).

In the case of sample A, the molecular interaction in the side chain structure of CF_3 is weaker than that in the straight chain structure of CF_2 because in CF_3, three-dimensional structures overlap and this leads to repulsion between fluorine atoms. Therefore, the damage due to exposure to X-ray during XPS measurement in the case of sample A is more than that in the case of sample B or that in the case of sample C. It is predicted that the trend observed in the adhesion properties of lubricants will be the same as that observed in the case of these damages. The water contact angle for each sample before and after the abrasion test is listed in table 2. Figs.6 - 8 show the phase image for each sample before and after abrasion test (image on the left: initial, image on the right: after abrasion test).

The results in table 2 indicate that the water contact angles in the case of sample B and sample C decreased slightly after the abrasion test was performed. In contrast, the water contact angle of sample A decreased drastically from 116° to 89° after the sample was scratched by a 2 kg weight over 600 strokes. In the case of sample A, it seems that the water repellant of lubricant was declined because it was decreased the lubricants quantity of sample A by abrasion test. A phase image that was obtained by AFM revealed the distribution of unevenness (roughness), the viscosity, elasticity, friction force, adhesion, and soft-hardness from the energy dissipation of interaction between tip and sample. In a previous study [12], we showed that the energy dissipation in the areas corresponding to bright areas in the phase image is greater than that in the areas corresponding to dark areas in the image. This result, along with a comparison of the phase image and force modulation image, reveals that the bright area is

softer or more adhesive than the dark area. Figs.6 - 8 show that the initial phase images of all the samples comprise a mixture of small soft areas and small hard areas (or small adhesive areas and small non-adhesive areas). In the case of sample A, a scratch is observed along the scan area in the image obtained after the abrasion test. Just like, the lubricants were removed by rubbing. Therefore, the water contact angle decreased when the lubricants were removed. On the other hand, in the case of sample B and sample C, we observed that the cluster of lubricants was larger than the initial cluster. Further, there is no scratch in the image obtained after the abrasion test. We guess that lubricants repeated the attaching & moving, the mixtures of soft regions and hard regions were grown by rubbing process. Thus, there is no significant change in the water contact angle. These results indicate that the trend in lubricant damage during XPS measurement agrees with the trend in durability during the abrasion test. Therefore, we found that we can select suitable lubricants for an ophthalmic lens by XPS measurement.

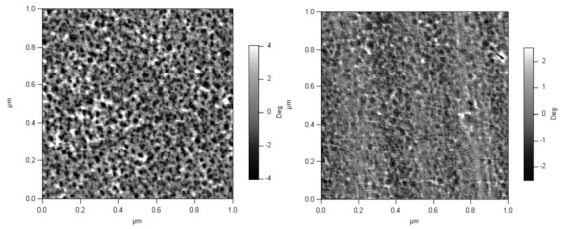

Fig.6. Phase image obtained for sample A (left image: initial, right image: after abrasion test).

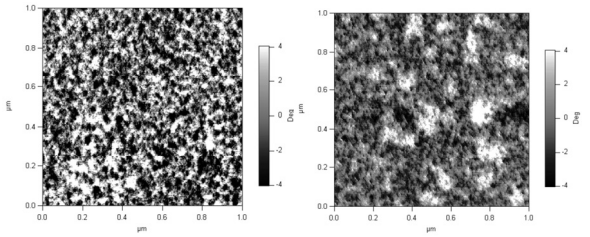

Fig.7. Phase image obtained for sample B (left image: initial, right image: after abrasion test).

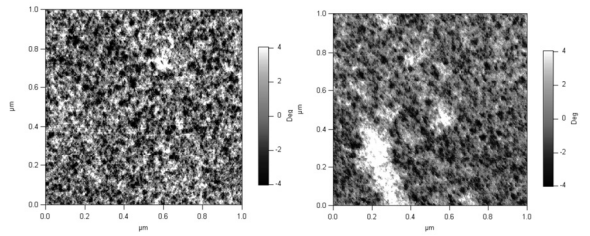

Fig.8. Phase image obtained for sample C (left image: initial, right image: after abrasion test).

Table 2. The water contact angle before and after the abrasion test.

	Initial	After abrasion test
Sample-A	116°	89°
Sample-B	110°	107°
Sample-C	111°	108°

4 Conclusions

We evaluated various methods for analyzing lubricants on ophthalmic lenses. The lubricant thickness can be directly determined by TEM measurement. The X-ray damage and the chemical structure can be investigated by XPS analysis and TOF-SIMS analysis. An abrasion test was carried out, and AFM phase images reveal the morphology of lubricants after the abrasion test. We suggest that the performance of X-ray damage by XPS is able to control the wear property of lubricants on the ophthalmic lens. This information can be used to improve the tribological performance of ophthalmic lenses in order to meet customer demand.

5 References

[1] C. M. Mate, M. R. Lorenz, and V. J. Novotny, J. Chem. Phys., vol.90,7550-7555 (1989).
[2] C. M. Mate and V. J. Novotny, J. Chem. Phys., vol.94, 8420-8427 (1991).
[3] M. F. Toney and C. M. Mate, IEEE.Trans.mag., vol.34, 1774-1776 (1991).
[4] V. J. Novotny, I. Hussla, J.-M. Turlet, and M. R. Philopott, J. Chem. Phys., 90 5861-5868 (1989).
[5] Y. Kimachi, F. Yoshimura, M. Hoshino, and A. Terada, IEEE.Trans.magn., vol.MAG-23, 2392-2394 (1987).
[6] N. Tadokoro and K. Osakabe, Rivista della Staz. Sper. Del Vetro n6, 155-158 (2000).
[7] H. Tani, IEEE.Trans.mag., vol.35, 2397-2399 (1999).
[8] Y. Sakane and M. Nakao, IEEE.Trans.mag., vol.35, 2394-2396 (1999).
[9] J. G. Newman and K. V. Viswanathan, J. Vac.Sci.Technol.A8 , 2388-2392 (1990).
[10] V. J. Novotny, X. Pan, and C. S. Bhatia, J. Vac.Sci.Technol.A12, 2879-2886 (1994).
[11]N. Tadokoro, S. Khraikratoke, P. Jamnongpian, A. Maeda, Y. Komine, N. Pavarinpong, S. Suyjantuk, and N. Iwata, Proc. World. Tribol. Congress 2009, 749 (2009).
[12] N. Tadokoro, S. Pannakarn, S. Khraikratoke, H. Kamura, and N. Iwata, Proc. the 8th ICCG8, 343-348 (2010).